Article

Cell Reports

DNAM-1 Expression Marks an Alternative Program of NK Cell Maturation

Graphical Abstract

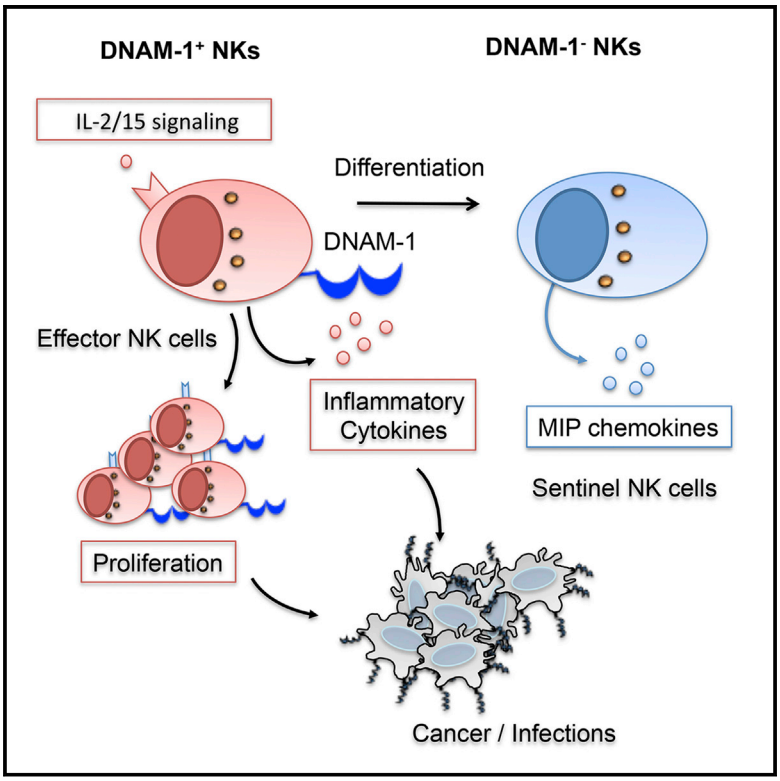

Authors

Ludovic Martinet,
Lucas Ferrari De Andrade, ...,
Nicholas D. Huntington, Mark J. Smyth

Correspondence

mark.smyth@qimrberghofer.edu.au

In Brief

Martinet et al. demonstrate that DNAM-1-activating receptor expression identifies two distinct subsets of natural killer (NK) cells. DNAM-1$^+$ NK cells proliferate vigorously, produce high levels of cytokines, and represent critical inflammatory and anti-tumor cells. By contrast, DNAM-1$^-$ NK cells that differentiate from DNAM-1$^+$ NK cells are higher producers of MIP1 chemokines.

Highlights

- The activating receptor DNAM-1 identifies two distinct NK cell functional subsets
- DNAM-1$^+$ NKs have enhanced IL-15 signaling and are a higher producer of cytokines
- DNAM-1$^-$ NKs are higher producers of MIP1 chemokines
- DNAM-1$^+$ NKs differentiate into DNAM-1$^-$ NKs through an alternative maturation pathway

Accession Numbers

GSE66281

Martinet et al., 2015, Cell Reports *11*, 85–97
April 7, 2015
http://dx.doi.org/10.1016/j.celrep.2015.03.006

Cell Reports
Article

DNAM-1 Expression Marks an Alternative Program of NK Cell Maturation

Ludovic Martinet,[1,2] Lucas Ferrari De Andrade,[1,3] Camille Guillerey,[1] Jason S. Lee,[4] Jing Liu,[1] Fernando Souza-Fonseca-Guimaraes,[1] Dana S. Hutchinson,[5] Tatiana B. Kolesnik,[6,7] Sandra E. Nicholson,[6,7] Nicholas D. Huntington,[6,7] and Mark J. Smyth[1,8,*]

[1]Immunology in Cancer and Infection Laboratory, QIMR Berghofer Medical Research Institute, Herston, QLD 4006, Australia
[2]Institut National de la Santé et de la Recherche Médicale (INSERM) UMR 1037, Cancer Research Center of Toulouse (CRCT), Toulouse 31000, France
[3]Células Inflamatórias e Neoplásicas group, Universidade Federal do Paraná, Curitiba, Paraná 81530-001, Brazil
[4]Control of Gene Expression Laboratory, QIMR Berghofer Medical Research Institute, Herston, QLD 4006, Australia
[5]Department of Pharmacology, Drug Discovery Biology, Monash Institute of Pharmaceutical, Sciences, Monash University, 399 Royal Parade, Parkville, VIC 3052, Australia
[6]The Walter and Eliza Hall Institute of Medical Research, Parkville, VIC 3050, Australia
[7]Department of Medical Biology, The University of Melbourne, Parkville, VIC 3010, Australia
[8]School of Medicine, University of Queensland, Herston, QLD 4006, Australia
*Correspondence: mark.smyth@qimrberghofer.edu.au
http://dx.doi.org/10.1016/j.celrep.2015.03.006

SUMMARY

Natural killer (NK) cells comprise a heterogeneous population of cells important for pathogen defense and cancer surveillance. However, the functional significance of this diversity is not fully understood. Here, we demonstrate through transcriptional profiling and functional studies that the activating receptor DNAM-1 (CD226) identifies two distinct NK cell functional subsets: DNAM-1$^+$ and DNAM-1$^-$ NK cells. DNAM-1$^+$ NK cells produce high levels of inflammatory cytokines, have enhanced interleukin 15 signaling, and proliferate vigorously. By contrast, DNAM-1$^-$ NK cells that differentiate from DNAM-1$^+$ NK cells have greater expression of NK-cell-receptor-related genes and are higher producers of MIP1 chemokines. Collectively, our data reveal the existence of a functional program of NK cell maturation marked by DNAM-1 expression.

INTRODUCTION

Natural killer (NK) cells are innate lymphocytes involved in the immune surveillance of cancer and the control of early infections (Spits et al., 2013; Vesely et al., 2011). NK cells express a wide range of activating and inhibitory receptors, allowing them to recognize and kill infected or transformed cells (Vivier et al., 2008). Upon activation, NK cells quickly produce various chemokines and cytokines such as MIP1α and MIP1β and IFN-γ, TNFα, IL-6, and GM-CSF, respectively (Colucci et al., 2003). This early source of inflammatory mediators alerts other immune components against potential dangers and provides a critical link between innate and adaptive immune responses (Raulet, 2004).

Despite some common features, NK cells represent a heterogeneous population of cells with diverse receptor repertoires and distinct maturation levels (Hayakawa et al., 2006). Several NK cell subsets with specialized functions have been described in humans and mice, suggesting that the functional diversity displayed by NK cells is governed by distinct NK cell subsets with discrete effector functions (Huntington et al., 2007a). In mice, two distinct populations of NK cells can be defined based on CD11b expression (Kim et al., 2002). CD11b$^-$ NK cells predominate in fetal and neonatal mice, display an "immature" phenotype, and demonstrate a high rate of homeostatic proliferation but poor cytotoxic functions. By contrast, the CD11b$^+$ NK cells represent the main mature subset in adult mice, express high levels of Ly49 receptors, and display higher cytotoxic functions compared to the CD11b$^-$ NK cells. NK cell development can be further divided using CD27 expression (Chiossone et al., 2009; Hayakawa and Smyth, 2006). In addition, the expression of KLRG1 on mature NK cells allows the identification of a terminal stage of NK cell differentiation associated with reduced proliferation and effector functions (Huntington et al., 2007b). Despite these advances, there is still extensive work required to characterize the different NK cell populations in mice and humans in regards to their specialized effector functions.

DNAM-1 (CD226) is an adhesion molecule triggering the cytotoxicity of NK and CD8$^+$ T cells upon interaction with its ligands CD155 and CD112 (Bottino et al., 2003; de Andrade et al., 2014; Shibuya et al., 1996). DNAM-1 receptor has been shown to be fundamental to NK-cell-dependent anti-tumor immunity (Chan et al., 2014; Gilfillan et al., 2008; Iguchi-Manaka et al., 2008; Lakshmikanth et al., 2009), and its role in other pathologies such as autoimmune disease (Huang et al., 2011) and infections (Cella et al., 2010) is also starting to emerge. Although DNAM-1 is homogeneously expressed on all T lymphocytes, this receptor is only expressed on approximately half of mouse splenic NK cells (Nabekura et al., 2014; Seth et al., 2009). Notably, the maturation status and phenotype of these two populations of NK cells were

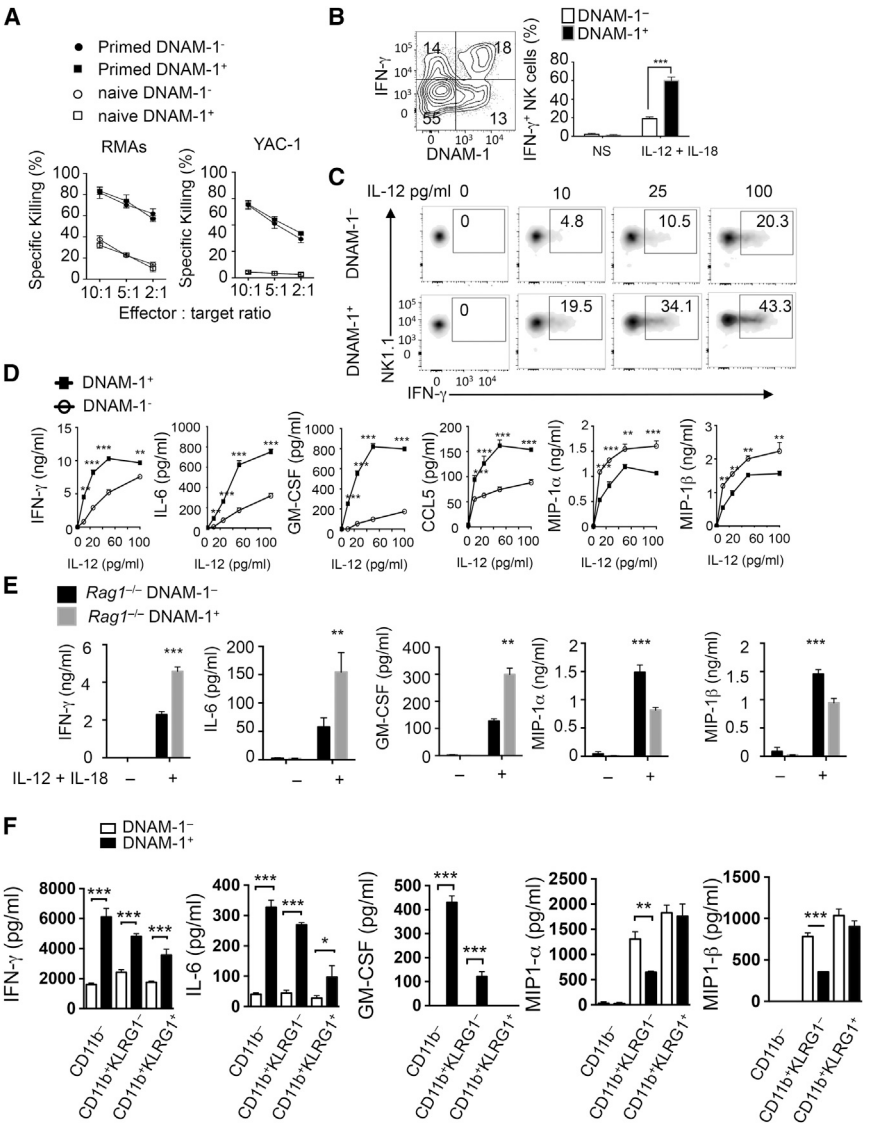

Figure 1. DNAM-1 Expression Identifies NK Cells with Distinct Cytokine-Secretion Profiles

(A) ^{51}Cr killing assay involving YAC-1 or RMAs targets incubated 4 hr at the indicated effector: target ratio with DNAM-1$^-$ or DNAM-1$^+$ NK cells freshly purified from the spleen of WT mice, naive, or primed for 24 hr with Poly I:C.

(B) Intracellular IFN-γ was analyzed in DNAM-1$^-$ and DNAM-1$^+$ fractions of purified spleen NK cells after stimulation with IL-12 (50 pg/ml) and IL-18 (50 ng/ml). The representative FACS plot (left) and the mean ± SD of triplicate wells (right) are shown.

(C and D) Representative FACS plot showing the intracellular IFN-γ content (C) and graph showing the concentrations of the indicated cytokines in the culture supernatants (D) of purified DNAM-1$^-$ and DNAM-1$^+$ NK cells stimulated with the indicated dose of IL-12 and IL-18 (50 ng/ml) for 24 hr.

(E) The concentrations of the indicated cytokines were analyzed in the supernatants of *Rag1*$^{-/-}$ DNAM-1$^-$ and DNAM-1$^+$ NK cells stimulated or not with IL-12 (25 pg/ml) and IL-18 (50 ng/ml) for 24 hr.

(F) CD11b$^-$, CD11b$^+$KLRG1$^-$, and CD11b$^+$KLRG1$^+$ NK cell subsets were sorted into DNAM-1$^-$ and DNAM-1$^+$ NK cells, and the concentrations of the indicated cytokines were analyzed in their culture supernatants after 24 hr in the presence of IL-12 (25 pg/ml) and IL-18 (50 ng/ml).

(A–F) Mean ± SD from triplicate wells; representative experiments of at least three independent experiments. *p < 0.05; **p < 0.01; ***p < 0.001; Student's t test.

reported to be similar, but until now, the origin and the functional role of DNAM-1$^-$ and DNAM-1$^+$ NK cells have been neglected. Here, we demonstrate that DNAM-1$^-$ and DNAM-1$^+$ NK cells possess distinct gene-expression profiles and functions. In addition, we provide evidence through the analysis of NK cell development that DNAM-1$^-$ NK cells develop from DNAM-1$^+$ NK cells independently of any known NK cell maturation scheme. Collectively, our data reveal the existence of a functional program of NK cell differentiation based on DNAM-1 expression.

RESULTS

DNAM-1 Expression Identifies NK Cells with Distinct Cytokine Secretion Profiles

Although the role of DNAM-1 receptor has been thoroughly investigated in tumor and infectious disease models (de Andrade et al., 2014), the biology of DNAM-1$^+$ and DNAM-1$^-$ NK cell populations remains poorly characterized. To address this question, we first investigated the killing capacities of both subsets in classical ^{51}Cr assays. We purified DNAM-1$^+$ and DNAM-1$^-$ NK cells from naive mice or primed in vivo with Poly I:C and found that the lysis of NKG2D-dependent targets YAC-1 and missing-self targets RMAs were similar between naive or primed DNAM-1$^-$ and DNAM-1$^+$ NK cells (Figure 1A). We next analyzed the intracellular production of IFN-γ by purified spleen NK cells after in vitro stimulation with IL-12 (50 pg/ml) and IL-18 (50 ng/ml). Surprisingly, we found that DNAM-1$^+$ NK cells produced significantly higher amounts of IFN-γ than DNAM-1$^-$ NK cells (Figure 1B). To confirm this result, we next stimulated purified DNAM-1$^-$ and DNAM-1$^+$ NK cells with different doses of IL-12 (10–200 pg/ml) and IL-18 (50 ng/ml). Regardless of the dose tested, DNAM-1$^+$ NK cells contained higher intracellular levels of IFN-γ than DNAM-1$^-$ NK cells (Figure 1C). We then performed a more-extensive screen of the cytokines and chemokines produced in the supernatants of DNAM-1$^-$ and DNAM-1$^+$ NK cells stimulated with IL-12 and IL-18. Critically, we found that the secretion profile differed between these two NK cell populations. DNAM-1$^+$ NK cells produced higher levels of IFN-γ, IL-6, GM-CSF, and

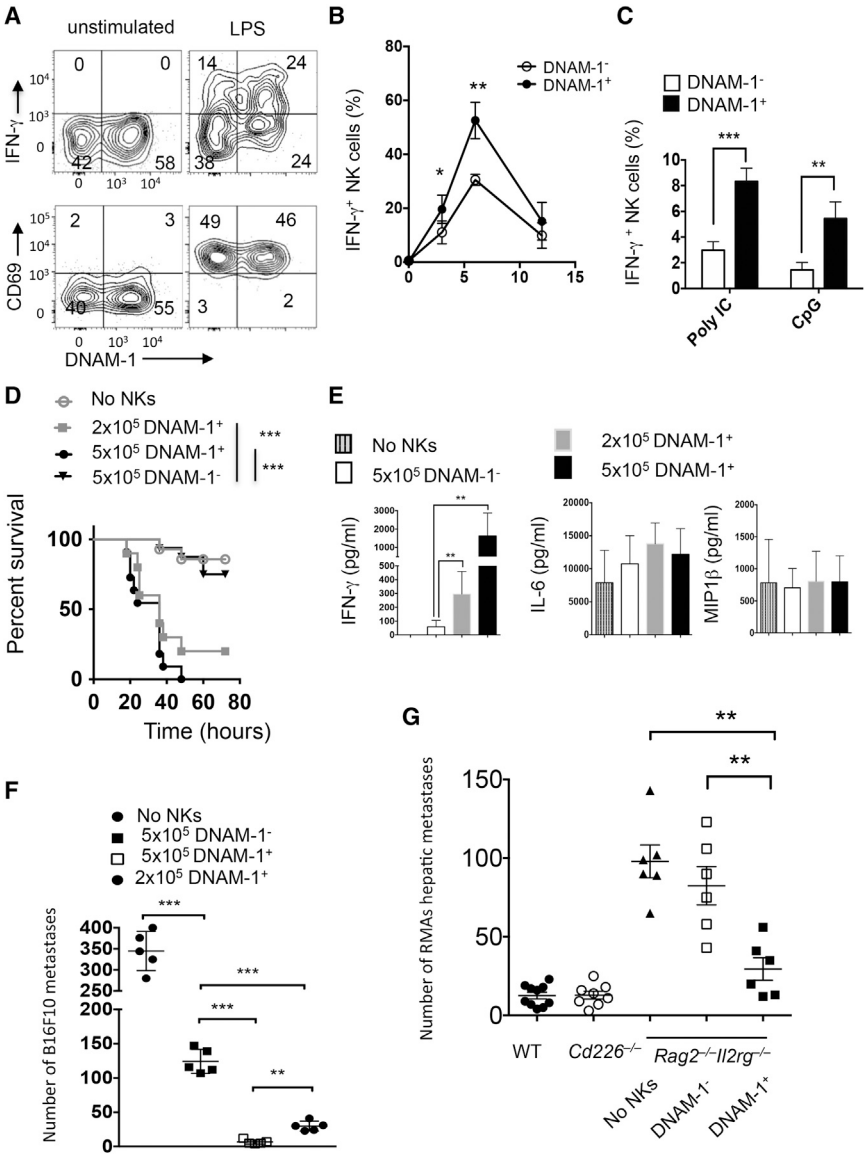

Figure 2. DNAM-1 Expression Identifies Pro-inflammatory and Anti-tumor NK Cells

(A) Representative FACS plot showing the intracellular production of IFN-γ and the expression of CD69 on DNAM-1$^-$ and DNAM-1$^+$ spleen NK cells 6 hr after in vivo LPS challenge.

(B) Graph showing the fraction of IFN-γ$^+$ DNAM-1$^-$ and DNAM-1$^+$ NK cells from WT mice 6 hr after LPS challenge. Mean ± SD from groups of five mice per time point is shown. Representative experiment of three performed.

(C) Graph showing the fraction of IFN-γ$^+$ DNAM-1$^-$ and DNAM-1$^+$ NK cells 12 hr after Poly I:C or CpG challenge. Mean ± SD from groups of five mice. Representative experiment out of two performed.

(D–G) *Rag2*$^{-/-}$*Il2rg*$^{-/-}$ mice were injected with PBS (No NKs) or with the indicated numbers of DNAM-1$^-$ and DNAM-1$^+$ NK cells. Five days later, peripheral blood NK cell reconstitution was analyzed and mice challenged with a lethal dose of LPS i.p. (0.5 mg/30 g mouse; D and E), with B16F10 melanoma cells (5 × 10^4 i.v.; F) or RMAs lymphoma (5 × 10^3 i.v.; G). Representative experiment of two using groups of five to ten mice.

(D and E) The survival was monitored over time (D), and the levels of IFN-γ, IL-6, and MIP-1α and β were quantified in the serum 12 hr after LPS challenge (E). Lungs (F) or liver (G) were collected 14 days after tumor injection, and the mean number metastases ± SEM are shown for each group of mice (crossbar) and individual mice represented by each symbol.

*p < 0.05; **p < 0.01; ***p < 0.001; Mann-Whitney test (B, C, E, F, and G) and Mantel-Cox test (D).

CCL5 whereas DNAM-1$^-$ NK cells produced higher amounts of MIP1α and MIP1β chemokines (Figure 1D). These distinct cytokine secretion profiles were also observed in culture of DNAM-1$^-$ and DNAM-1$^+$ NK cells stimulated with other cytokine cocktails (Figure S1). Similar results were obtained with DNAM-1$^+$ and DNAM-1$^-$ NK cells purified from *Rag1*$^{-/-}$, *TCRδ*$^{-/-}$, or CD3ε$^{-/-}$ mice (Figures 1E and S1), excluding any role for T cell contaminants (Stewart et al., 2007).

Consistent with previous reports (Nabekura et al., 2014; Seth et al., 2009), we observed that DNAM-1$^+$ and DNAM-1$^-$ NK cells have a classical NK cell phenotype and express similar maturation markers (Figure S1). Yet, to exclude the influence of previously defined maturation markers, we assessed cytokine secretion in response to IL-12 and IL-18 stimulation from CD11b$^-$, CD11b$^+$KLRG1$^-$, and CD11b$^+$KLRG1$^+$ DNAM-1$^-$ and DNAM-1$^+$ NK cell subsets (Figure 1F). Although the secretion of some cytokines such as GM-CSF or MIP1α and β were specific to distinct maturation stages, the profile of cytokine secretion of DNAM-1$^+$ and DNAM-1$^-$ NK cells was consistent throughout NK cell maturation as defined by these subsets (Figure 1F). Collectively, these results demonstrate that DNAM-1 expression allows a new functional separation of NK cells independently of the previously defined maturation markers.

DNAM-1 Expression Identifies Pro-inflammatory and Anti-tumor NK Cells

To gain more insight into the functional role of DNAM-1$^-$ and DNAM-1$^+$ NK cell subsets in vivo, we next analyzed DNAM-1$^-$ and DNAM-1$^+$ NK cell responses during TLR-ligand-driven inflammation. After lipopolysaccharide (LPS) injection, we detected a significantly higher percentage of IFN-γ-producing cells in the DNAM-1$^+$ versus DNAM-1$^-$ fraction of NK cells, although both populations expressed similar levels of CD69 activation marker (Figures 2A and 2B). Similar observations were made using other TLR ligands. Twelve hours after injecting Poly I:C (TLR3 agonist) or CpG DNA (TLR9 agonist), we observed that DNAM-1$^+$ NK cells contained a higher

fraction of IFN-γ-producing cells than DNAM-1$^-$ NK cells (Figure 2C).

To better appreciate the pathophysiological functions of DNAM-1$^-$ and DNAM-1$^+$ NK cells in vivo, we transferred purified DNAM-1$^-$ or DNAM-1$^+$ NK cells into *Rag2*$^{-/-}$*Il2rg*$^{-/-}$ mice and analyzed the endotoxicosis shock syndrome induced by challenge with a high dose of LPS (Anthony et al., 2010). After LPS challenge, mice reconstituted with 2 × 10^5 or 5 × 10^5 DNAM-1$^+$ NK cells succumbed significantly faster than mice reconstituted with 5 × 10^5 DNAM-1$^-$ NK cells, whereas non-reconstituted mice all survived LPS injection (Figures 2D and S2). Twelve hours after LPS stimulation, serum levels of IFN-γ were significantly higher in mice transferred with DNAM-1$^+$ NK cells than in mice transferred with DNAM-1$^-$ NK cells (Figure 2E). Mice that did not receive any NK cells had undetectable IFN-γ production in response to LPS. By contrast, all the different groups of mice had similar levels of non-NK-cell-specific cytokines (Figure 2E). Similar results were obtained using DT-treated *Nkp46*^{iCre}*R26R*^{DTR}, which allows the conditional ablation of NK cells (Walzer et al., 2007), reconstituted with purified DNAM-1$^-$ or DNAM-1$^+$ NK cells (Figure S2).

To extend our knowledge of the anti-tumor functions of distinct NK cell subsets in vivo, we transferred DNAM-1$^+$ NK cells and DNAM-1$^-$ NK cells into *Rag2*$^{-/-}$*Il2rg*$^{-/-}$ mice that were subsequently challenged with the highly metastatic B16F10 melanoma cell line. We found that DNAM-1$^+$ NK cells had superior anti-metastatic functions to DNAM-1$^-$ NK cells. Even low numbers of DNAM-1$^+$ NK cells were sufficient to clear most if not all B16F10 metastases, whereas more than 100 metastases were still present on the lungs of mice injected with DNAM-1$^-$ NK cells (Figures 2F and S2). Given that host DNAM-1 is critical to the suppression of B16F10 lung metastases (Gilfillan et al., 2008), this result was not unexpected. To confirm these results, we assessed the anti-tumor functions of DNAM-1$^+$ and DNAM-1$^-$ NK cells using survival (i.p.) and hepatic metastasis (i.v.) models of RMAs, which expresses CD155 but is cleared equivalently by WT and *Cd226*$^{-/-}$ (DNAM-1-deficient) mice (Figure S2). We found that purified DNAM-1$^+$ NK cells were more effective at controlling RMAs tumor growth and experimental metastasis than DNAM-1$^-$ NK cells when transferred into lymphocyte-deficient *Rag2*$^{-/-}$*Il2rg*$^{-/-}$ mice (Figures 2G and S2). Collectively, these results demonstrate that DNAM-1$^+$ NK cells are critical effector cells during TLR-ligand-driven inflammation and tumor suppression in vivo.

DNAM-1$^+$ NK Cell Functions Do Not Depend on DNAM-1 and CD155 Interactions

Recent reports indicate that the differential binding of CD96, T cell receptor with Ig and ITIM domains (TIGIT), and DNAM-1 to CD155 impacts on NK cell function (Chan et al., 2014; Stanietsky et al., 2013). To determine whether increased CD96 and TIGIT signaling in the absence of DNAM-1 may account for the differences observed between DNAM-1$^-$ and DNAM-1$^+$ NK cells, we sorted DNAM-1$^+$ and DNAM-1$^-$ NK cell populations from *Tigit*$^{-/-}$ and *Cd96*$^{-/-}$ mice. Upon cytokine stimulation, DNAM-1$^+$ NK cells produced higher levels of inflammatory cytokines, regardless of the presence or absence of TIGIT and CD96 (Figures 3A and 3B). We next tried to understand the role of DNAM-1 and CD155 interactions in the differential functions of DNAM-1$^-$ and DNAM-1$^+$ NK cells. DNAM-1$^-$ and DNAM-1$^+$ NK cells were stimulated in the presence or absence of anti-DNAM-1 mAb (480.1; 10 μg/ml; Chan et al., 2014) to assess the functional role of DNAM-1 in the cytokine secretion by DNAM-1$^-$ and DNAM-1$^+$ NK cells. Surprisingly, DNAM-1 blockade did not alter the profile of cytokine production by DNAM-1$^+$ and DNAM-1$^-$ NK cells (Figure 3C). Similar results were obtained when DNAM-1$^+$ and DNAM-1$^-$ NK cells were stimulated in the presence of anti-CD155 mAb (4.24.3; 10 μg/ml; Chan et al., 2014) or when CD155$^{-/-}$ NK cells were used to block the interaction of DNAM-1 with its major ligand CD155 (Figures 3C and 3D). These results suggest that the functional differences between DNAM-1$^-$ and DNAM-1$^+$ NK cells are not a direct consequence of co-stimulatory signals provided by DNAM-1 engagement but may rather result from genetic differences in these populations.

DNAM-1 Expression Is Associated with a Distinct Gene-Expression Profile

Therefore, to better understand the origin of the functional differences between DNAM-1$^-$ and DNAM-1$^+$ NK cell subsets, we analyzed their gene-expression patterns by microarray profiling. A total of 561 and 305 genes were significantly over- and under-expressed in DNAM-1$^+$ NK cells compared to DNAM-1$^-$ NK cells (corrected t test $p < 0.05$), demonstrating that DNAM-1$^+$ and DNAM-1$^-$ NK cells have distinct gene profiles (Figures 4A, 4B, and S3). These belonged to several functional families including transcription factors, cytokines and chemokines, cell cycle, adhesion molecules, and NK cell receptors (NKRs). DNAM-1$^-$ NK cells mainly overexpressed genes related to NKR signaling such as *Klra* family genes *Cd247*, *Lat2*, *Zap70*, and *Prk* (Figure 4C). Molecular network analysis revealed that NFκB and PKC networks were the two main molecular networks upregulated in DNAM-1$^-$ NK cells (Figure S4). IL-21 and TNF-α were among the top five transcriptional regulators associated with the observed gene-expression changes in DNAM-1$^-$ NK cells (Figure S4). DNAM-1$^+$ NK cells expressed higher levels of cytokine-related genes, consistent with their pro-inflammatory profile (Figure 4C). Overall DNAM-1$^+$ NK cells appeared to display a more-activated phenotype than their DNAM-1$^-$ counterparts.

DNAM-1 Expression Is Associated with a More-Active IL-15 Receptor Pathway

Molecular network analysis revealed that E2F and cytokine-signaling networks were the two main molecular networks upregulated in DNAM-1$^+$ NK cells (Figures 5A and S4). Interestingly, a number of genes found upregulated in these two networks are directly linked to the common IL-2- and IL-15-receptor-signaling pathway. The signaling through this receptor is pivotal for the maturation and the acquisition of effector functions of NK cells (Huntington et al., 2007a). Differences in IL-15 receptor signaling may explain the functional division between DNAM-1$^+$ and DNAM-1$^-$ NK cells. To confirm this hypothesis, we analyzed the phosphorylation of key transduction molecules involved in IL-15-receptor-signaling pathways. We observed higher levels of phosphorylated JAK1 and STAT5A/B upon IL-15 stimulation of DNAM-1$^+$ NK cells, compared to the IL-15 response in

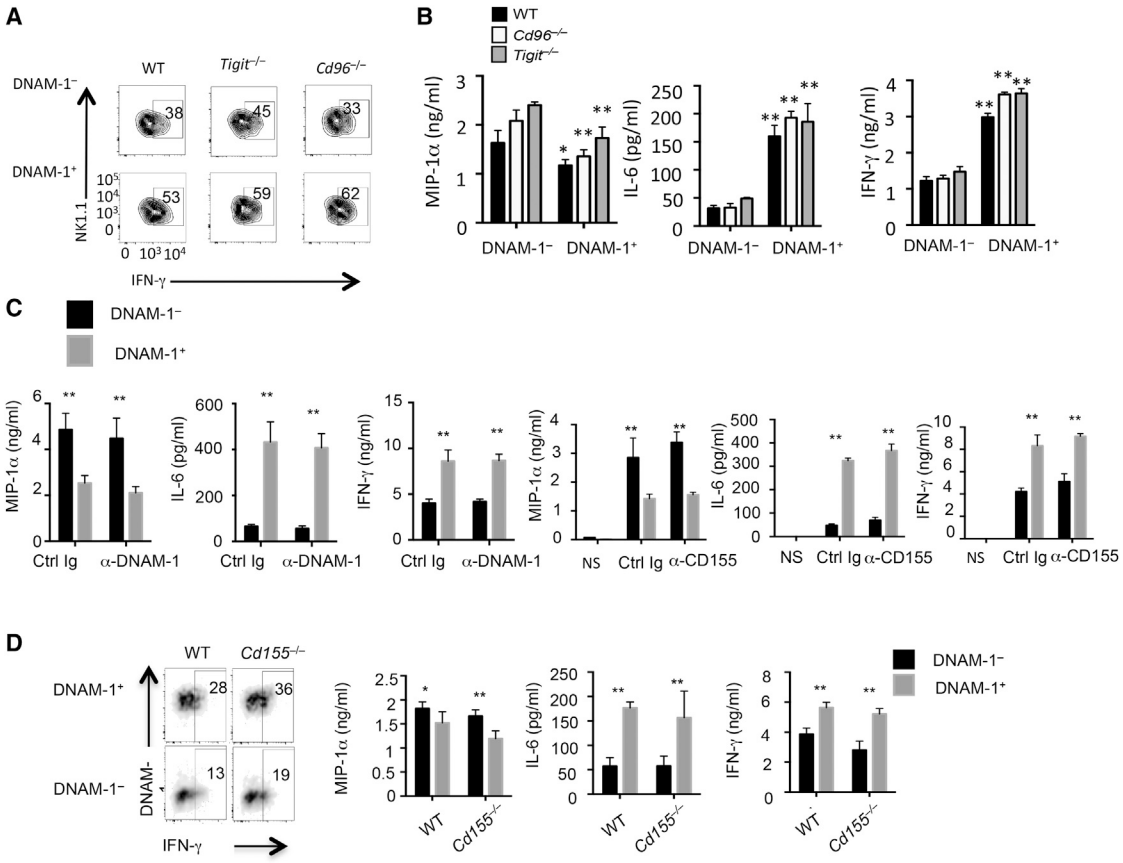

Figure 3. DNAM-1$^-$ and DNAM-1$^+$ NK Cell Functions Do Not Depend on DNAM-1 and CD155 Interactions

(A and B) FACS-sorted DNAM-1$^-$ and DNAM-1$^+$ NK cells from WT, *Tigit*$^{-/-}$, and *Cd96*$^{-/-}$ mice were stimulated with IL-12 (25 pg/ml) and IL-18 (50 ng/ml). The representative FACS plot showing the intracellular IFN-γ content (A) and the mean ± SD concentration of the indicated cytokines from triplicate wells (B) from one representative experiment out of three are shown.

(C) FACS-sorted DNAM-1$^-$ and DNAM-1$^+$ NK cells were stimulated with IL-12 (25 pg/ml) and IL-18 (50 ng/ml) in the presence of control Ig (Ctrl Ig), anti-CD155, or anti-DNAM-1. The mean ± SD from triplicate wells from one representative experiment of three independent experiments is shown.

(D) Representative FACS plot showing the intracellular IFN-γ content (left) and graph showing the concentrations of the indicated cytokines in the culture supernatants (right) of purified *Cd155*$^{-/-}$ and WT DNAM-1$^-$ and DNAM-1$^+$ NK cells stimulated with IL-12 and IL-18 for 24 hr. The mean ± SD from triplicate wells from one representative experiment of three independent experiments is shown.

n.s., $p > 0.05$; *$p < 0.05$; **$p < 0.01$; Student's t test.

DNAM-1$^-$ NK cells (Figures 5B and S5). In addition, higher levels of phosphorylated MEK1/2 were detected in DNAM-1$^+$ NK cells upon IL-15 stimulation, demonstrating that the IL-15-receptor-mediated MAPK-signaling pathway is also enhanced in DNAM-1$^+$ NK cells (Figure 5B). Collectively, these results demonstrate that DNAM-1$^+$ NK cells are characterized by increased IL-15 receptor signaling.

Recent studies indicate the existence of a positive feedback loop between IL-15 signaling and the serine threonine kinase mTOR (mammalian target of rapamycin) (Marçais et al., 2014). IL-15-mediated activation of mTOR was shown to stimulate NK cell metabolism to increase IL-15 receptor expression and was required for IL-15-dependent effector functions. Upon IL-15 stimulation, we detected higher level of phosphorylation of mTORC1 downstream targets rsp6 (ribosomal protein S5) in DNAM-1$^+$ NK cells (Figure 5B). However, the levels of phosphorylation of mTORC2 downstream target Akt1 (Ser437) were similar in both subsets (Figure S5). In addition, we could not detect critical differences in the metabolic activity of DNAM-1$^-$ and DNAM-1$^+$ NK cells using seahorse technology and found that the oxygen consumption rate (OCR) and extracellular acidification rate (ECAR) were not significantly different between both subsets (Figure S5).

DNAM-1 Expression Identifies NK Cells with Distinct Proliferative Response

IL-15 receptor is critically involved in NK cell proliferation, and we found that a number of genes related to E2F network involved in cell cycle, cell death, and survival were upregulated in DNAM-1$^+$ NK cells (Figures 5A, S3, and S4). These results prompted us to investigate the proliferative response of DNAM-1$^-$ and DNAM-1$^+$ NK cells. Freshly sorted DNAM-1$^-$ and DNAM-1$^+$ NK cells were labeled with Cell Trace Violet (CTV) and cultured in vitro with IL-2 or IL-15. We observed that DNAM-1$^+$ NK cells proliferated more

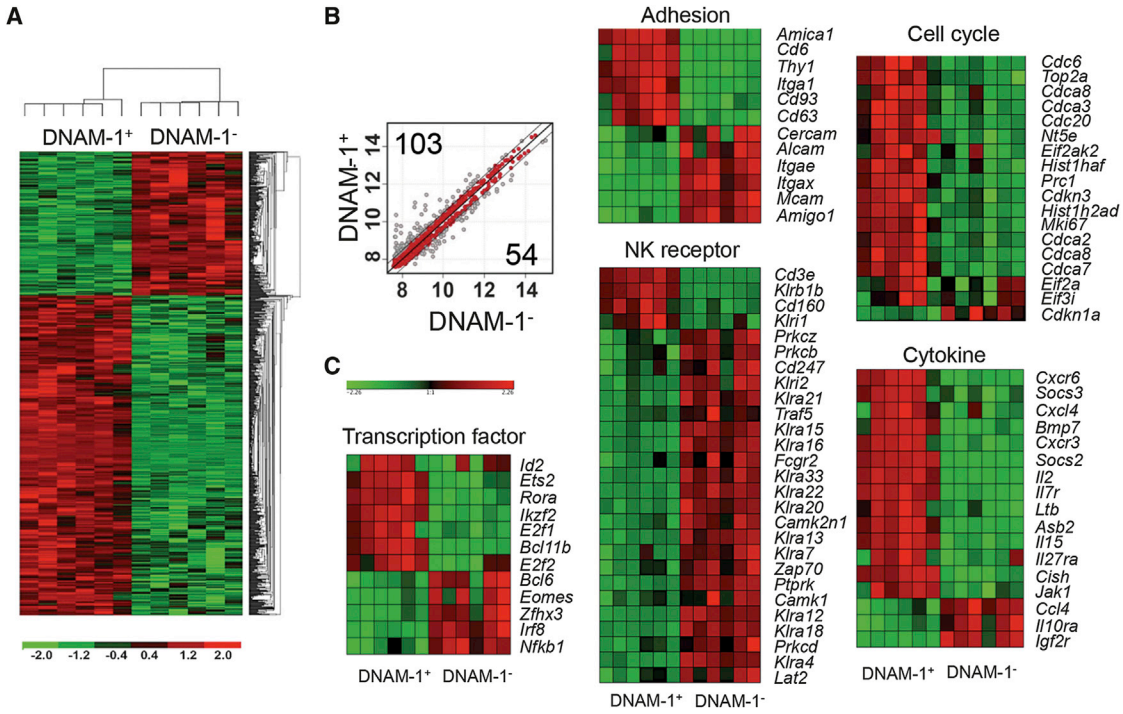

Figure 4. DNAM-1 Expression Is Associated with a Distinct Gene-Expression Profile

(A) Heatmap and unsupervised hierarchical clustering of DNAM-1$^+$ and DNAM-1$^-$ NK cells genes (six independent samples are shown for each population).

(B) Comparison plots of normalized expression values. Numbers indicate genes whose expression differed by more than 1.5-fold between DNAM-1$^+$ and DNAM-1$^-$ NK cells. Differentially expressed genes are highlighted in gray ($p < 0.05$ unpaired t test).

(C) Heatmap of genes related to transcription factors, cell cycle, cytokines and chemokines, cellular adhesion, and NK cell receptor signaling differentially expressed ($p < 0.05$ unpaired t test) between DNAM-1$^+$ and DNAM-1$^-$ NK cells (six independent samples from each population are shown).

vigorously than DNAM-1$^-$ NK cells in response to IL-2 and IL-15, confirming the enhanced sensitivity of DNAM-1$^+$ NK cells for these two cytokines (Figure 6A). To investigate NK cell proliferation in vivo, we transferred DNAM-1$^-$ and DNAM-1$^+$ NK cells from adult mice into *Rag2*$^{-/-}$*Il2rg*$^{-/-}$ mice. Analysis of NK cell reconstitution revealed that DNAM-1$^+$ NK cells have higher homeostatic expansion capacities than DNAM-1$^-$ NK cells. Indeed, up to 4 weeks after injection, we recovered higher NK cell numbers and percentages in *Rag2*$^{-/-}$*Il2rg*$^{-/-}$ mice transferred with DNAM-1$^+$ NK cells than in mice transferred with DNAM-1$^-$ NK cells (Figures 6B and S6). Analysis of NK cell proliferation 5 days after cell transfer into *Rag2*$^{-/-}$*Il2rg*$^{-/-}$ mice through CTV dilution revealed that DNAM-1$^+$ NK cells undergo higher number of divisions than DNAM-1$^-$ NK cells (Figures 6C and S6). We confirmed the superior proliferative potential of DNAM-1$^+$ NK cells over DNAM-1$^-$ NK cells by injecting both subsets simultaneously into *Rag2*$^{-/-}$*Il2rg*$^{-/-}$ (Figure 6D).

The depletion of Tregs was previously shown to induce the production of IL-2 by conventional T cells, leading to the massive expansion of NK cells (Gasteiger et al., 2013). We took advantage of the *Foxp3*^{DTR} mice to analyze the IL-2-induced proliferation of DNAM-1$^-$ and DNAM-1$^+$ NK cells in vivo. The depletion of Tregs with DT for 5 days increased the fraction of Ki67$^+$-proliferating cells in both DNAM-1$^-$ and DNAM-1$^+$ NK cell populations compared to PBS treatment (Figure 6E). However, a significantly higher fraction of Ki67$^+$-proliferating cells was detected in the DNAM-1$^+$ fraction of NK cells (Figures 6E and 6F). As a consequence, the numbers and the percentages of DNAM-1$^+$ NK cells were selectively enriched in the spleen of mice treated for 5 days with DT as compared to PBS-treated mice (Figures 6F and 6G). Together, these results indicate that DNAM-1 expression identifies NK cells with a greater ability to proliferate under lymphopenic conditions or following cytokine stimulation.

DNAM-1$^-$ NK Cells Arise from DNAM-1$^+$ NK Cells through an Alternative Maturation Program

Given the critical differences between DNAM-1$^-$ and DNAM-1$^+$ NK cells, we wanted to address the developmental origin of these two NK cell populations. We first purified splenic DNAM-1$^-$ and DNAM-1$^+$ NK cells from adult mice that were subsequently transferred into *Rag2*$^{-/-}$*Il2rg*$^{-/-}$ mice. Analysis of DNAM-1 expression 2–8 weeks after injection revealed that DNAM-1$^-$ NK cells have a stable phenotype in vivo (Figure 7A). By contrast, we saw a progressive emergence of DNAM-1$^-$ NK cells over time in the *Rag2*$^{-/-}$*Il2rg*$^{-/-}$ mice injected with DNAM-1$^+$ NK cells (Figure 7A). Similar results were obtained when purified DNAM-1$^-$ and DNAM-1$^+$ NK cells were cultured in vitro with IL-2 (Figure S7).

We next analyzed the relationship between these two populations during the neonatal emergence of NK cells. Interestingly, we observed that most of the NK cells were DNAM-1$^+$ 10 days after birth, with the DNAM-1$^-$ population being almost

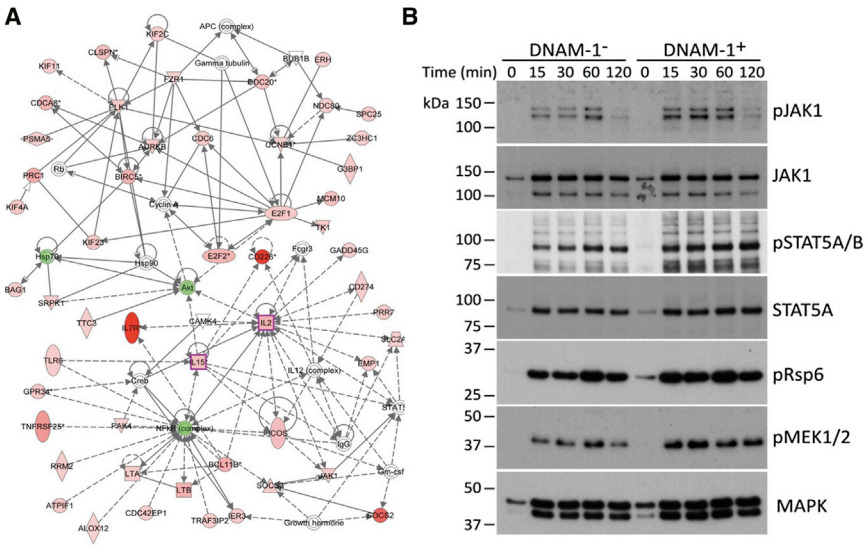

Figure 5. DNAM-1 Expression Is Associated with a More-Active IL-15 Receptor Pathway

(A) Molecular network analysis of DNAM-1$^+$ upregulated genes. Cell-cycle and cytokine-signaling networks were generated from the microarray analysis of genes differentially expressed between DNAM-1$^+$ and DNAM-1$^-$ NK cells. Red represents upregulation, and green represents downregulation. Numbers indicate fold change of gene expression. E2F network (upper diagram) shows that 28 genes related to cell cycle, cell death and survival, cellular assembly, and organization were upregulated in DNAM-1$^+$ NK cells. Cytokine-signaling network (lower diagram) shows that 27 focus molecules involved in cell-mediated immune response, cellular development, cellular functions, and maintenance were upregulated in DNAM-1$^+$ NK cells.

(B) Purified DNAM-1$^-$ or DNAM-1$^+$ NK cells were stimulated with IL-15 (5 ng/ml) for 0, 15, 30, 60, or 120 min. Western blots using antibodies directed against the indicated total and phosphorylated (p) proteins are shown. Representative experiment out of two performed.

undetectable (Figure 7B). During the first 60 days after birth, the percentage and the number of DNAM-1$^-$ NK cells progressively increased to reach similar number and percentages to the DNAM-1$^+$ population (Figures 7B–7D). We observed concomitant changes in CD11b$^-$ immature and mature CD11b$^+$CD27$^+$ and CD11b$^+$CD27$^-$NK cell subsets (Figure 7C). However, DNAM-1$^-$ NK cell development was independent of CD27/CD11b NK cell maturation scheme because immature and mature NK cells subsets were similarly represented in DNAM-1$^-$ and DNAM-1$^+$ NK cells throughout NK cell neonatal development (Figure S7). We next used the *Nkp46*^{iCre}*R26R*^{DTR} mice to analyze in adult mice the kinetics of DNAM-1$^-$ and DNAM-1$^+$ NK cell subset recovery after diphtheria toxin (DT)-induced NK cell depletion. As observed for neonatal NK cells, most of the newly generated NK cells were DNAM-1$^+$ whereas DNAM-1$^-$ developed later (Figure 7E). These results suggest that DNAM-1$^-$ NK cells develop from DNAM-1$^+$ NK cells rather than from separate precursors. To confirm this assumption, we purified DNAM-1$^+$ NK cells from 10-day-old WT mice and transferred them into *Rag2*$^{-/-}$*Il2rg*$^{-/-}$ mice. We observed a progressive differentiation of the transferred immature DNAM-1$^+$ NK cells into mature DNAM-1$^+$ and DNAM-1$^-$ NK cells (Figure 7F).

To determine whether the differentiation of DNAM-1$^+$ NK cells into DNAM-1$^-$ is restricted to a specific NK cell stage, we next sorted immature CD11b$^-$, mature CD11b$^+$KLRG1$^-$, and terminally differentiated CD11b$^+$KLRG1$^+$ NK cells into DNAM-1$^+$ and DNAM-1$^-$ populations and transferred them into *Rag2*$^{-/-}$*Il2rg*$^{-/-}$ mice. Interestingly, we observed that DNAM-1$^+$ could differentiate into DNAM-1$^-$ NK cells at any stage of maturation (Figure 7G). By contrast, regardless of the maturation stage, DNAM-1$^-$ retained their DNAM-1$^-$ phenotype, confirming the inability of these cells to re-express DNAM-1 (Figure 7G). These results confirm that DNAM-1 allows the identification of two splenic NK cell subsets independently of the known maturation markers: DNAM-1$^+$ and DNAM-1$^-$ NK cells.

DISCUSSION

Here, we demonstrated through the analysis of NK cell development, transcriptional profiling, and functional studies that the activating receptor DNAM-1 regulates an alternative program of differentiation to generate two distinct NK cell functional subsets: DNAM-1$^+$ and DNAM-1$^-$ NK cells. DNAM-1$^+$ NK cells had enriched expression of IL-15-signaling-related genes, proliferated vigorously, produced high levels of effector cytokines, and represented critical effector cells during inflammatory and anti-tumor reactions. In contrast, DNAM-1$^-$ NK cells had a greater expression of NKR-related genes and were higher producers of MIP1 chemokines. Finally, we provided strong evidence that DNAM-1$^-$ NK cells represent a stable subset that differentiates from DNAM-1$^+$ NK cells independently of the classical NK cell maturation pathway. Collectively, our data reveal the existence of a new functional program of NK cell differentiation based on DNAM-1 expression.

Defective Ly49H$^+$ NK cell memory responses to MCMV were recently described in the absence of DNAM-1. DNAM-1 ligands were induced during MCMV infection, and the engagement of DNAM-1 on NK cells was required for optimal MCMV clearance. Because experiments conducted in this study were performed using gene-targeted mice and blocking antibodies, the intrinsic functions and properties of DNAM-1$^+$ and DNAM-1$^-$ NK cells were not investigated (Nabekura et al., 2014). By contrast, in our study, we provide strong evidence that DNAM-1$^-$ and DNAM-1$^+$ NK cells represent distinct NK cell subsets with divergent functions. Nabekura et al. (2014) demonstrated that Ly49H$^+$ and DNAM-1$^+$ NK cells lose DNAM-1 expression during the course of infection. However, because approximately half of mouse NK cells are DNAM-1$^-$ in steady state (uninfected), regardless of the expression of Ly49H (Seth et al., 2009), the relationship between DNAM-1$^-$ and DNAM-1$^+$ NK cells was unclear. In our work, through the analysis of NK cell development and adoptive transfer experiments using sorted neonatal or adult

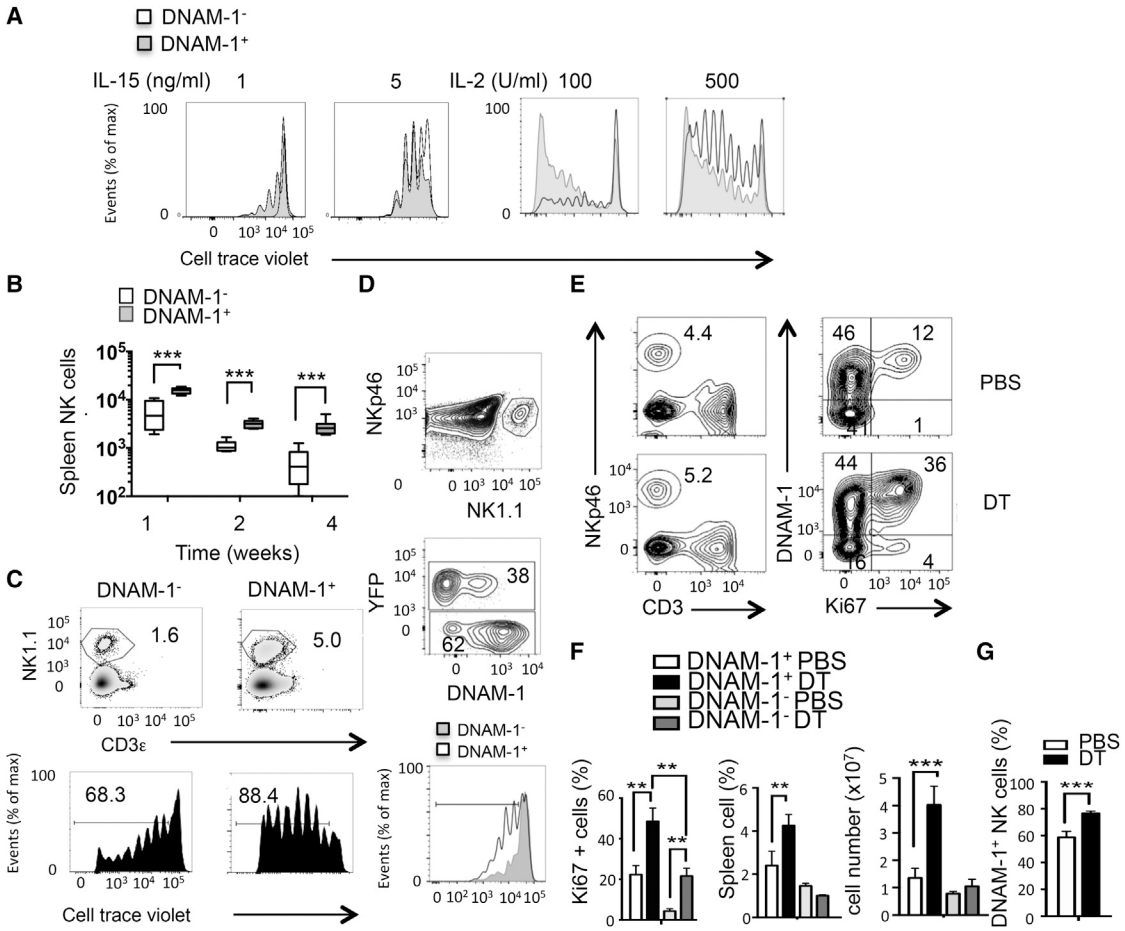

Figure 6. DNAM-1 Expression Identifies NK Cells with Distinct Proliferative Capacities

(A) Representative FACS histograms showing the proliferation of Cell-Trace-Violet-labeled DNAM-1$^-$ (white histogram) or DNAM-1$^+$ NK cells (gray histogram) stimulated with the indicated concentration of IL-2 or IL-15 for 5 days. Representative experiment out of three performed.

(B) Box plots showing the total number of spleen NK cells recovered 1, 2, or 4 weeks after DNAM-1$^-$ or DNAM-1$^+$ NK cell injection into *Rag2*$^{-/-}$*Il2rg*$^{-/-}$ mice. Data are pooled from at least two independent experiments involving groups of six to ten mice per time point.

(C) Representative FACS plots showing the total percentage among spleen cells (upper panel) and the percentage of divided NK1.1$^+$CD3$^-$ NK cells (lower panel) 5 days after injection into *Rag2*$^{-/-}$*Il2rg*$^{-/-}$ mice. Representative experiment of three performed.

(D) Cell-Trace-Violet-labeled DNAM-1$^+$ and DNAM-1$^-$ NK cells were sorted from WT and *Nkp46*^{iCre}*R26R*^{eYFP}, respectively, and transferred simultaneously into *Rag2*$^{-/-}$*Il2rg*$^{-/-}$ mice. Representative FACS plots showing the total percentage (central panel) and the percentage of divided DNAM-1$^-$ (YFP$^+$) and DNAM-1$^+$ (YFP$^-$) NK cells (lower panel) 5 days after injection. Representative experiment out of two performed.

(E–G) The expansion of DNAM-1$^-$ and DNAM-1$^+$ NK cells was analyzed in BALB/c *Foxp3*^{DTR} mice 5 days after treatment with DT or PBS vehicle. (E and F) Representative density plots (E) and graphs (F) showing the percentage of Ki67$^+$ cells, the percentage among spleen cells, and the total number of spleen DNAM-1$^-$ and DNAM-1$^+$ fractions of NK cells after Treg depletion or not. (G) Graph showing the percentage of NK cells expressing DNAM-1 after Treg depletion or not. (F and G) Mean ± SD from a representative experiment of two independent experiments involving groups of five mice.

(B, F, and G) **p < 0.01; ***p < 0.001; Mann-Whitney test.

NK cells, we demonstrated that DNAM-1$^-$ NK cells develop from DNAM-1$^+$ NK cells. Interestingly, the differentiation of DNAM-1$^+$ into DNAM-1$^-$ NK cells was not restricted to a particular subset of DNAM-1$^+$ NK cells because both immature CD11b$^-$ and mature NK cells progressively differentiated into DNAM-1$^-$ NK cells when transferred into lymphopenic hosts. Surprisingly, the results of Nakebura and colleagues (Nabekura et al., 2014) suggest that DNAM-1$^-$ Ly49H$^+$ NK cells are also plastic and can change their DNAM-1 phenotype during the course of infection. However, in contrast with Nabekura et al., our experiments demonstrate that DNAM-1$^-$ NK cells are not plastic and represent a final stage of NK cell differentiation. Perhaps DNAM-1 may be acquired by membrane exchange (trogocytosis) between NK cells and APCs that can express DNAM-1 (Joly and Hudrisier, 2003). Another possibility is contamination by DNAM-1$^+$ NK cells in the DNAM-1$^-$ NK cell fraction that would expand during the course of MCMV infection.

The molecular determinants controlling the differentiation of DNAM-1$^+$ into DNAM-1$^-$ NK cells remain to be fully understood. One possibility is that DNAM-1 interaction with CD155 might down-modulate the expression of DNAM-1. We analyzed DNAM-1 expression in *Cd155*$^{-/-}$ mice and found that the ratio

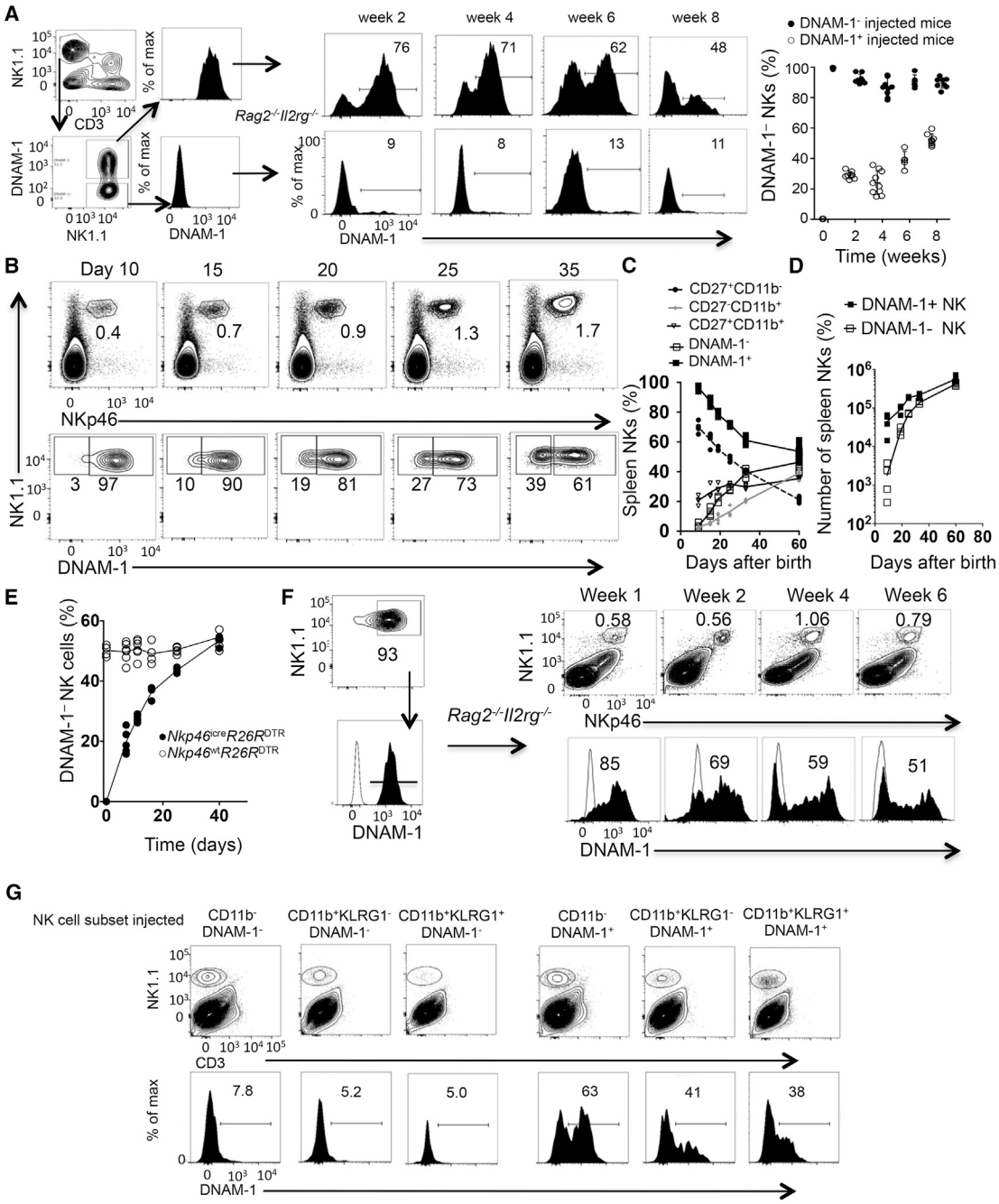

Figure 7. DNAM-1$^-$ NK Cells Differentiate from DNAM-1$^+$ NK Cells

(A) Purified DNAM-1$^-$ or DNAM-1$^+$ NK cells were transferred into *Rag2*$^{-/-}$*Il2rg*$^{-/-}$ mice. Representative histogram (left panel) or graph (right panel) showing DNAM-1 expression on spleen NK cells isolated 2–8 weeks after injection.

(B–D) Representative density plots and graphs showing the percentage (B and C) and number (D) of the indicated WT spleen NK cell subsets during neonatal development. Representative experiment of two involving groups of three to ten mice per time point.

(E) The percentage of DNAM-1$^-$ spleen NK cells was analyzed in *Nkp46*^{iCre}*R26R*^{DTR} or *Nkp46*^{WT}*R26R*^{DTR} mice after DT injection. Experiment involving groups of four to six mice per time point.

(F) Purified spleen DNAM-1$^+$ NK cells from 10-day-old WT mice were transferred into *Rag2*$^{-/-}$*Il2rg*$^{-/-}$ mice, and DNAM-1 expression was analyzed on spleen NK cells 1–6 weeks after injection. Representative histograms showing the expression of DNAM-1 (black histogram) compared to isotype control staining (open histogram) from experiments involving five to ten mice per time point are shown.

(G) CD11b$^-$, CD11b$^+$KLRG1$^-$, and CD11b$^+$KLRG1$^+$ NK cells were sorted into DNAM-1$^+$ and DNAM-1$^-$ NK cell populations and transferred into *Rag2*$^{-/-}$*Il2rg*$^{-/-}$ mice. Three weeks after transfer, DNAM-1 expression was analyzed on spleen NK1.1$^+$CD3$^-$ NK cells. A representative experiment of two involving five mice per time point is shown.

of DNAM-1$^+$ and DNAM-1$^-$ NK cells was consistent with WT mice, demonstrating that CD155 is not involved in the loss of DNAM-1 expression (Figure S7). As already demonstrated by other groups (Seth et al., 2009), we observed that mRNAs for DNAM-1 were almost absent in DNAM-1$^-$ NK cells compared to DNAM-1$^+$. This suggests there must be a strong repression of the DNAM-1 gene occurring in DNAM-1$^-$ NK cells that is independent of ligand binding. NK cell differentiation is often preceded by a proliferation stage, and blocking NK cell proliferation also blocks NK cell maturation (Marçais et al., 2014). Analysis of DNAM-1$^-$ differentiation in vitro during the course of NK cell proliferation revealed that the emergence of DNAM-1$^-$ NK cells was mainly confined to NK cells that had undergone several rounds of division (Figure S7). This raises the question as to whether DNAM-1$^-$ NK cells may differentiate from DNAM-1$^+$ NK cells upon the stochastic loss of DNAM-1 expression during NK cell proliferation. IL-15 plays a pivotal role in the progression of immature NK cells toward more-mature NK cell stages (Huntington et al., 2009; Vosshenrich et al., 2005). For example, a reduction in IL-15 signaling blunts the development of NK cells at the CD11b$^-$ stage and, conversely, increased IL-15 concentrations induce the accumulation of KLRG1$^+$ NK cells (Huntington et al., 2007b, c; Lee et al., 2011). IL-15 receptor downstream signals may control the differentiation of DNAM-1$^-$ NK cells because DNAM-1$^-$ NK cells have less-active IL-15 signaling and IL-15 stimulates DNAM-1 expression.

Transcriptional analysis of DNAM-1$^-$ and DNAM-1$^+$ NK cells revealed that these two subsets have distinct gene signatures. Interestingly, a number of genes overexpressed in DNAM-1$^+$ NK cells were directly related to IL-15 signaling. In accordance with the mitogenic and anti-apoptotic properties of this cytokine (Fehniger et al., 2001; Gilmour et al., 2001; Huntington et al., 2007c), numbers of cell-cycle- and survival-related genes were also specifically increased in DNAM-1$^+$ NK cells. Analysis of IL-15 signaling confirmed that DNAM-1$^+$ NK cells have a more active IL-15-signaling pathway with higher levels of JAK1 and STAT5 phosphorylation upon IL-15 stimulation. Given the pivotal role played by this cytokine in controlling diverse aspects of NK cell biology, such as proliferation and acquisition of effector functions, it is likely that such differences in IL-15 reactivity account for the divergent functions of DNAM-1$^-$ and DNAM-1$^+$ NK cells. The molecular basis for enhanced IL-15 signaling remains to be fully understood. Indeed, we could not detect any substantial differences in the cell surface expression of IL-15Rβ (CD122) and common γc chain (CD132) between DNAM-1$^-$ and DNAM-1$^+$ NK cells, and IL-15-mediated activation of the PI3K-Akt-signaling cascade was similar between these two NK subsets.

DNAM-1 is an adhesion molecule originally shown to control NK and T cell cytotoxicity upon interaction with its ligands CD155 and CD112, which are frequently upregulated upon cellular transformation (Bottino et al., 2003; Shibuya et al., 1996). This receptor seems to play a broader role than initially thought in NK cell biology because recent studies indicate that DNAM-1 also controls immune synapse formation, cytokine secretion, and memory NK cell differentiation (Chan et al., 2014; de Andrade et al., 2014; Nabekura et al., 2014; Ramsbottom et al., 2014). In addition to these functions, here, we demonstrate that DNAM-1 separates NK cells in two functional subsets. Interestingly, we found that blocking DNAM-1/ligand interactions during functional assays using *Cd155*$^{-/-}$ NK cells or anti-CD155 and anti-DNAM-1 mAbs did not alter DNAM-1$^-$- and DNAM-1$^+$-related functions. These results suggest that DNAM-1 engagement does not directly account for the functional differences between these two NK cell subsets but rather may be involved in the epigenetic control of DNAM-1$^+$ NK cell identity. We can speculate that cellular interactions and signals provided to DNAM-1$^-$ and DNAM-1$^+$ NK cells might be different, ultimately leading to functional divergence. Indeed, DNAM-1 at the cell surface of lymphocytes constantly interacts with its ligands expressed on DCs (Seth et al., 2011), and the absence of this receptor has been shown to negatively impact NK cell and DC crosstalk (Pende et al., 2006; Ramsbottom et al., 2014; Shibuya et al., 1996). The absence of DNAM-1 on NK cells may therefore limit their access to homeostatic DC-derived signals including IL-15 (Lucas et al., 2007). Thus, NK cell/DC crosstalk defects in the absence of DNAM-1 may underlie the lower IL-15 reactivity of DNAM-1$^-$ NK cells.

DNAM-1$^+$ and DNAM-1$^-$ NK cells greatly differed in their expression of adhesion molecules and their NKR repertoire. Genes coding for NKR (Ly49D, G, H, and M) and NKR-signaling molecules (LAT, ZAP70, and PKC) were among the most-upregulated genes in DNAM-1$^-$ NK cells. These results contrast with the increased expression of genes related to cytokine signaling in DNAM-1$^+$ NK cells and suggest that DNAM-1$^-$ NK cell reactivity may be controlled by NKR-derived cellular signals whereas DNAM-1$^+$ reactivity may be controlled by accessory cell-derived cytokines. Although this idea is attractive, we could not find clear evidence demonstrating enhanced NKR reactivity in DNAM-1$^-$ NK cells. For example, the in vitro lysis of YAC-1 and RMAs was similar between DNAM-1$^-$ and DNAM-1$^+$ NK cells, demonstrating equal missing-self and NKG2D-dependent killing. By contrast, DNAM-1$^+$ NK cells had superior anti-tumor functions to DNAM-1$^-$ NK cells in vivo. It will be most interesting to confirm the role of these subsets using CD155$^-$ tumor cell lines, because virtually all of the mouse tumor cell lines of solid or hematological origin express some or significant levels of CD155.

Although mouse and human NK cells exert similar functions and share some common developmental pathways, their phenotype greatly differs between these two species, making translational discovery difficult (Huntington et al., 2007a). Mouse NK cells are mainly separated based on their expression of CD11b and CD27, whereas human NK cells are dichotomized based on the level of expression of the CD56 adhesion molecule. CD56^{bright} NK cells proliferate vigorously and produce high amount of inflammatory mediators in response to exogenous cytokine stimulation, whereas CD56^{dim} effector functions are mainly elicited by NKR triggering (Cooper et al., 2001a, b; Fauriat et al., 2010). DNAM-1$^+$ and DNAM-1$^-$ NK cell global gene-expression profiles and functional attributes suggest these cells may represent the mouse analogs of human CD56^{bright} and CD56^{dim} NK cells. Similar to human CD56^{bright} and CD56^{dim} NK cell subsets (Cooper et al., 2001b), we found increased levels of DNAM-1$^+$ NK cells in peripheral lymph nodes and in the BM, whereas DNAM-1$^-$ NK cells were more prevalent in the blood and in the lung. Although most human peripheral blood NK cells express DNAM-1 (El-Sherbiny et al., 2007), several studies

revealed the presence of a population of NK cells with lower DNAM-1-receptor expression in cancer patients (Carlsten et al., 2009; Mamessier et al., 2011; Sanchez-Correa et al., 2012). Constant ligand exposure was found to support DNAM-1 down-modulation, and accumulating evidence suggests that loss of DNAM-1 expression is associated with a decrease in NK cell function (Carlsten et al., 2009; Mamessier et al., 2011). Until now, it remains unclear whether these NK cells have a stable phenotype and could represent the equivalent of mouse DNAM-1$^-$ NK cells. A better understanding of the role of DNAM-1 on NK cell behavior may therefore have future therapeutic application in cancer patients.

EXPERIMENTAL PROCEDURES

Mice

BALB/c and C57BL/6 wild-type mice were obtained from the Walter and Eliza Hall Institute for Medical Research or ARC Animal Resource Centre. *Rag1*$^{-/-}$, *Rag2*$^{-/-}$*Il2rg*$^{-/-}$, *Cd226*$^{-/-}$, and *Cd96*$^{-/-}$ have been described (Chan et al., 2014). *Nkp46*^{iCre}*R26R*^{eYFP} and *Nkp46*^{iCre}*R26R*^{DTR} mice were kindly provided by Dr. Eric Vivier (Narni-Mancinelli et al., 2011). *Tigit*$^{-/-}$ mice were provided by Bristol Myers Squibb. *Cd155*$^{-/-}$ mice were kindly provided by Dr. Yoshimi Takai (Kobe University). BALB/c *Foxp3*^{DTR} mice were provided by Dr. Alexander Rudensky (Kim et al., 2007). All mice were bred and maintained at the QIMR Berghofer Medical Research Institute and were used at the age of 6–12 weeks. Group sizes were designed to ensure adequate power for the detection of biological differences. No mice were excluded on the basis of pre-established criteria, and no active randomization was applied to experimental groups. The investigators were not "blinded" to group allocation during the experiment and/or when assessing the outcome. All experiments were approved by QIMR Berghofer Medical Research Institute animal ethics committees.

^{51}Cr Cytotoxicity Assays

The B16F10 melanoma cell line, RMAs, and YAC-1 lymphoma cell lines (all from American Type Culture Collection) were grown at 37°C in 5% CO_2 in complete RPMI medium (e.g., supplemented with 10% FCS [Thermo Scientific], L-glutamine, nonessential amino acids, sodium pyruvate, HEPES, and penicillin-streptomycin [all GIBCO]). Standard ^{51}Cr cytotoxicity assays were used to measure the ability of DNAM-1$^-$ and DNAM-1$^+$ NK cells to kill targets. NK cells were added to ^{51}Cr-labeled targets at defined effector-to-target ratios. After 4 hr at 37°C in 5% CO_2, supernatants were harvested, and the level of ^{51}Cr was quantified by a gamma counter (Chan et al., 2010).

Treg and NK Cell Depletion

Tregs were depleted from BALB/c *Foxp3*^{DTR} mice by successive i.p. injection of DT (200 ng/30 g of body weight; Merck) at days 0, 2, and 4. Mice were sacrificed at day 5 to analyze the expansion of spleen DNAM-1$^-$ and DNAM-1$^+$ NK cells and depletion of Foxp3$^+$ T cells. NK cells were depleted from *Nkp46*^{iCre}*R26R*^{DTR} mice by two successive daily injections i.p. of DT (8 ng/g of body weight; Merck). Littermates *Nkp46*^{WT}*R26R*^{DTR} control mice were included in each experiment. The depletion of retro-orbital sinus blood NKp46$^+$ NK cells was determined prior to each experiment.

NK Cell Purification and Activation

NK cells were enriched from the spleens of the appropriate strains of mice by MACS technology (NK cells isolation kit II; Miltenyi Biotec), using an autoMACS pro separator (Miltenyi Biotec). Enriched NK cells preparations were then stained with mAb to NK1.1 (PK136; eBioscience), mAb to TCRβ (H57-597; eBioscience), mAb to CD3 (17A2; eBioscience), mAb to NKp46 (29A1.4; BioLegend), and mAb to DNAM-1 (480.1; BioLegend), and DNAM-1$^-$ or DNAM-1$^+$ NK cells were sorted on a FACSAria II (BD Biosciences). NK cells were labeled with CTV (Life Technologies) according to the manufacturer's instructions. Freshly purified NK cells were plated in 96-well U-bottomed plates in complete RMPI medium supplemented with the indicated concentrations of recombinant human IL-2 (100–1,000 U/ml; Chiron), mouse IL-12 (25–100 pg/ml; eBioscience), mouse IL-15-IL-15Rα (1–100 ng/ml; eBioscience), and mouse IL-18 (50 ng/ml; R&D Systems). The production of cytokines was analyzed in the supernatant and in NK cells after 24 hr of culture, whereas the proliferation of NK cells was analyzed after 5 days of culture. Where indicated, mAb to DNAM-1 (10 μg/ml; 480.1), mAb to CD155 (10 μg/ml; 4.24.3), or irrelevant IgG1 (HRPN; Bio X cell) was added.

TLR Ligand Challenge

LPS (from *Escherichia coli* strain 0127:B8; Sigma) suspended in PBS was injected i.p. into mice at various doses (0.1 mg and 0.5 mg per 30 g mouse body weight). TLR3 agonist Poly (I:C) (100 μg; Sigma) and TLR9 agonist CpG DNA (100 μg; Sigma) were injected i.v. For adoptive transfer experiments, DNAM-1$^-$ or DNAM-1$^+$ NK cells (2–5 × 10^5) freshly purified from WT mice were injected via the tail vein of *Rag2*$^{-/-}$*Il2rg*$^{-/-}$ mice or DT-treated *Nkp46*^{iCre}*R26R*^{DTR} mice. The NK cell reconstitution was analyzed 5 days later and mice were challenged by i.p. injection of LPS (0.5 mg/30 g mouse). Blood was obtained 12 hr after TLR ligand injection from the retro-orbital sinuses, and the serum was used for cytokine analysis. Spleens were obtained from mice at various time points for analysis of receptor expression and intracellular expression of IFN-γ by NK cells. For survival experiments, mice were checked hourly for signs of sepsis.

Flow Cytometry and Cytokine Detection

Cells harvested from in vitro cultures or single-cell suspensions from various organs were incubated for 15 min in Fc-blocking buffer (2.4G2). Cells were then stained with the appropriate antibodies from eBioscience (mAb to CD3 [17A2], mAb to CD69 [H1.2F3], mAb to NK1.1 [PK136], mAb to TCRβ [H57-597], mAb to Ki67 [SolA15], or mAb to KLRG1 [2F1]) or from BioLegend (mAb to DNAM-1 [480.1], mAb to CD11b [M1/70], or mAB to NKp46 [29A1.4]). Data were acquired with an LSR II Fortessa (BD Biosciences) and were analyzed with FlowJo software (TreeStar). All cytokines were detected by cytometric bead array technology according to the manufacturer's instructions (BD Biosciences). For detection of intracellular cytokines, splenocytes from TLR-ligand-injected mice or in-vitro-activated NK cells were stained, fixed, and permeabilized with Cytofix/Cytoperm (BD Biosciences) and then were stained with an anti-IFN-γ mAb (XMG1.2; BD Biosciences).

Tumor Assays

DNAM-1$^-$ or DNAM-1$^+$ NK cells (2–5 × 10^5) were injected via the tail vein into *Rag2*$^{-/-}$*Il2rg*$^{-/-}$ mice. The reconstitution of each mouse by NK cells was analyzed 5 days later in the peripheral blood by flow cytometry, and mice were then given an intravenous injection of B16F10 melanoma cells (5 × 10^4) or RMAs lymphoma cells (5 × 10^3). Lungs or livers, respectively, were collected after 14 days, and B16F10 or RMAs tumor nodules were counted under a dissection microscope (Chan et al., 2010). Survival of mice injected with the RMAs lymphoma cells i.p. (5 × 10^2) was monitored.

DNAM-1$^-$ and DNAM-1$^+$ NK Cell Homeostasis

Two hundred thousand DNAM-1$^-$ or DNAM-1$^+$ NK cells labeled with CTV were injected via the tail vein into *Rag2*$^{-/-}$*Il2rg*$^{-/-}$ mice. The proliferation, the percentage, the number, and DNAM-1 expression were analyzed on transferred NK cells in the spleen of each mouse 5 days to 8 weeks after injection. To analyze the neonatal expansion of DNAM-1$^-$ or DNAM-1$^+$ NK cells, 10- to 100-day-old C57BL/6 WT mice were sacrificed and the percentage, the number, and DNAM-1 expression on spleen NK cells were determined by flow cytometry. Alternatively, some experiments were conducted on DT-treated *Nkp46*^{iCre}*R26R*^{DTR} mice to analyze DNAM-1 expression during NK cell recovery in adult mice.

Microarray

The total RNA was extracted from purified DNAM-1$^-$ or DNAM-1$^+$ NK cells using RNeasy micro kit (QIAGEN). The integrity and the quantity of the RNA were evaluated using 2100 Bioanalyzer (Agilent Technologies). Using the Illumina TotalPrep RNA Amplification Kit (Ambion), 300 ng of RNA were reverse transcribed into cRNA and thereby labeled with biotin-UTP. Hybridization of 1,500 ng of labeled cRNA to the Illumina mouse WG-6 v2.0 Expression Beadchip array was followed by washing steps as described in the protocol.

Microarray analysis was performed according to manufacturer's instructions. Student's t test was used to determine differentially expressed genes between samples. Multiple testing corrections were used to adjust p values derived from multiple tests.

Molecular Network Analysis

Differentially expressed genes identified from the microarray analysis comparing DNAM-1$^+$ and DNAM-1$^-$ NK cells were used. The molecular network was algorithmically constructed by Ingenuity Pathway Analysis (IPA) software (QIAGEN) on the basis of the functional and biological links between genes. Gene-expression data are overlaid on the network to show up- and downregulated genes as red and green, respectively.

Seahorse Assay

XF96 cell culture microplates (Seahorse Bioscience) were first coated with 0.1% gelatin for 30 min at 37°C before the addition of 2 × 10^5 DNAM1$^{+/-}$ NK cells in unbuffered glucose-free DMEM. NK cells were stimulated with glucose (25 mM), oligomycin (1 μM), FCCP (1.5 M) plus pyruvate (1 mM), and antimycin A (1 μM) plus rotenone (0.1 μM) with ECAR and OCR being measured every 7 min for 105 min by an XF-96 Extracellular Flux Analyzer (Seahorse Bioscience).

Western Blot Analysis

One million DNAM-1$^-$ or DNAM-1$^+$ NK cells were stimulated in complete RPMI supplemented with IL-2 (500 U/ml) or IL-15 (5 ng/ml) for 0, 15, 30, or 60 min. Cells were harvested and lysed in RIPA buffer (300 mM NaCl, 2% IGEPAL CA-630, 1% deoxycholic acid, 0.2% SDS, and 100 mM Tris-HCl [pH 8.0]) with protease inhibitors (Roche Diagnostics), 1 mM sodium orthovanadate (Sigma), and 10 mM sodium fluoride. About 30 μg of protein was loaded into NuPAGE 10% Bis-Tris gels. Western blots were probed with the following antibodies: α-P-STAT5a/b (Tyr$^{694/699}$; Millipore), α-STAT5a (Zymed) α-P-JAK1 (Tyr$^{1022/1023}$; Invitrogen), α-JAK1 (HR-785; 1:1,000; Santa Cruz), α-P-Akt1 (Ser^{473}; Cell Signaling Technology), α-P-MEK1/2 (Ser$^{217/221}$; Cell Signal), α-P-p42/44 MAPK (Tyr $^{202/204}$; Cell Signal), α-P-rsp6 (Ser$^{235/236}$; Cell Signal), and α-β-actin-HRP (Santa Cruz Biotechnology). Antibody binding was visualized with horseradish-peroxidase-conjugated secondary antibodies: sheep anti-rabbit immunoglobulin or sheep anti-mouse immunoglobulin (GE Healthcare) and the enhanced chemiluminescence (ECL) system (Millipore) or Amersham ECL (GE Healthcare). To re-blot, membranes were first stripped of antibodies in 0.1 M glycine (pH 2.9).

Statistical Analysis

Statistical analysis was achieved using Graphpad Prism Software. Data were compared by an unpaired Student's t test when values followed a Gaussian distribution with similar variances or with the Mann Whitney test. Differences in survival were evaluated with a Mantel-Cox test.

ACCESSION NUMBERS

The full microarray data set has been deposited in Gene Expression Omnibus (GEO) under submission number GSE66281.

SUPPLEMENTAL INFORMATION

Supplemental Information includes seven figures and can be found with this article online at http://dx.doi.org/10.1016/j.celrep.2015.03.006.

AUTHOR CONTRIBUTIONS

All authors contributed to the experiments in this manuscript. L.M., N.D.H., and MJ.S. designed the study and wrote the manuscript.

ACKNOWLEDGMENTS

The authors thank Liam Town, Joanne Sutton, and Kate Elder for the care and maintenance of the mouse colonies. We thank Fiona Amante, Marcela Montes De Oca, Christian Engwerda, and Fares Al-Ejeh for their technical and scientific help. M.J.S. is supported by a NHMRC Australia Fellowship (628623). L.M. is supported by the ARC Cancer Research Foundation. D.S.H. was supported by a NHMRC Career Development Fellowship. The project was supported by NHMRC program grants (1013667 and 1016647) and project grants (1044392, 1049407, 1066770, and 1057852) and was supported in part by an NHMRC IRIISS grant 361646 and a Victorian State Government Operational Infrastructure Scheme grant.

Received: October 15, 2014
Revised: December 31, 2014
Accepted: February 27, 2015
Published: March 26, 2015

REFERENCES

Anthony, D.A., Andrews, D.M., Chow, M., Watt, S.V., House, C., Akira, S., Bird, P.I., Trapani, J.A., and Smyth, M.J. (2010). A role for granzyme M in TLR4-driven inflammation and endotoxicosis. J. Immunol. *185*, 1794–1803.

Bottino, C., Castriconi, R., Pende, D., Rivera, P., Nanni, M., Carnemolla, B., Cantoni, C., Grassi, J., Marcenaro, S., Reymond, N., et al. (2003). Identification of PVR (CD155) and Nectin-2 (CD112) as cell surface ligands for the human DNAM-1 (CD226) activating molecule. J. Exp. Med. *198*, 557–567.

Carlsten, M., Norell, H., Bryceson, Y.T., Poschke, I., Schedvins, K., Ljunggren, H.G., Kiessling, R., and Malmberg, K.J. (2009). Primary human tumor cells expressing CD155 impair tumor targeting by down-regulating DNAM-1 on NK cells. J. Immunol. *183*, 4921–4930.

Cella, M., Presti, R., Vermi, W., Lavender, K., Turnbull, E., Ochsenbauer-Jambor, C., Kappes, J.C., Ferrari, G., Kessels, L., Williams, I., et al.; CHAVI Clinical Core B; NIAID Center for HIV/AIDS Vaccine Immunology (2010). Loss of DNAM-1 contributes to CD8+ T-cell exhaustion in chronic HIV-1 infection. Eur. J. Immunol. *40*, 949–954.

Chan, C.J., Andrews, D.M., McLaughlin, N.M., Yagita, H., Gilfillan, S., Colonna, M., and Smyth, M.J. (2010). DNAM-1/CD155 interactions promote cytokine and NK cell-mediated suppression of poorly immunogenic melanoma metastases. J. Immunol. *184*, 902–911.

Chan, C.J., Martinet, L., Gilfillan, S., Souza-Fonseca-Guimaraes, F., Chow, M.T., Town, L., Ritchie, D.S., Colonna, M., Andrews, D.M., and Smyth, M.J. (2014). The receptors CD96 and CD226 oppose each other in the regulation of natural killer cell functions. Nat. Immunol. *15*, 431–438.

Chiossone, L., Chaix, J., Fuseri, N., Roth, C., Vivier, E., and Walzer, T. (2009). Maturation of mouse NK cells is a 4-stage developmental program. Blood *113*, 5488–5496.

Colucci, F., Caligiuri, M.A., and Di Santo, J.P. (2003). What does it take to make a natural killer? Nat. Rev. Immunol. *3*, 413–425.

Cooper, M.A., Fehniger, T.A., and Caligiuri, M.A. (2001a). The biology of human natural killer-cell subsets. Trends Immunol. *22*, 633–640.

Cooper, M.A., Fehniger, T.A., Turner, S.C., Chen, K.S., Ghaheri, B.A., Ghayur, T., Carson, W.E., and Caligiuri, M.A. (2001b). Human natural killer cells: a unique innate immunoregulatory role for the CD56(bright) subset. Blood *97*, 3146–3151.

de Andrade, L.F., Smyth, M.J., and Martinet, L. (2014). DNAM-1 control of natural killer cells functions through nectin and nectin-like proteins. Immunol. Cell Biol. *92*, 237–244.

El-Sherbiny, Y.M., Meade, J.L., Holmes, T.D., McGonagle, D., Mackie, S.L., Morgan, A.W., Cook, G., Feyler, S., Richards, S.J., Davies, F.E., et al. (2007). The requirement for DNAM-1, NKG2D, and NKp46 in the natural killer cell-mediated killing of myeloma cells. Cancer Res. *67*, 8444–8449.

Fauriat, C., Long, E.O., Ljunggren, H.G., and Bryceson, Y.T. (2010). Regulation of human NK-cell cytokine and chemokine production by target cell recognition. Blood *115*, 2167–2176.

Fehniger, T.A., Suzuki, K., Ponnappan, A., VanDeusen, J.B., Cooper, M.A., Florea, S.M., Freud, A.G., Robinson, M.L., Durbin, J., and Caligiuri, M.A. (2001). Fatal leukemia in interleukin 15 transgenic mice follows early

expansions in natural killer and memory phenotype CD8+ T cells. J. Exp. Med. *193*, 219–231.

Gasteiger, G., Hemmers, S., Bos, P.D., Sun, J.C., and Rudensky, A.Y. (2013). IL-2-dependent adaptive control of NK cell homeostasis. J. Exp. Med. *210*, 1179–1187.

Gilfillan, S., Chan, C.J., Cella, M., Haynes, N.M., Rapaport, A.S., Boles, K.S., Andrews, D.M., Smyth, M.J., and Colonna, M. (2008). DNAM-1 promotes activation of cytotoxic lymphocytes by nonprofessional antigen-presenting cells and tumors. J. Exp. Med. *205*, 2965–2973.

Gilmour, K.C., Fujii, H., Cranston, T., Davies, E.G., Kinnon, C., and Gaspar, H.B. (2001). Defective expression of the interleukin-2/interleukin-15 receptor beta subunit leads to a natural killer cell-deficient form of severe combined immunodeficiency. Blood *98*, 877–879.

Hayakawa, Y., and Smyth, M.J. (2006). CD27 dissects mature NK cells into two subsets with distinct responsiveness and migratory capacity. J. Immunol. *176*, 1517–1524.

Hayakawa, Y., Huntington, N.D., Nutt, S.L., and Smyth, M.J. (2006). Functional subsets of mouse natural killer cells. Immunol. Rev. *214*, 47–55.

Huang, Z., Fu, B., Zheng, S.G., Li, X., Sun, R., Tian, Z., and Wei, H. (2011). Involvement of CD226+ NK cells in immunopathogenesis of systemic lupus erythematosus. J. Immunol. *186*, 3421–3431.

Huntington, N.D., Vosshenrich, C.A., and Di Santo, J.P. (2007a). Developmental pathways that generate natural-killer-cell diversity in mice and humans. Nat. Rev. Immunol. *7*, 703–714.

Huntington, N.D., Tabarias, H., Fairfax, K., Brady, J., Hayakawa, Y., Degli-Esposti, M.A., Smyth, M.J., Tarlinton, D.M., and Nutt, S.L. (2007b). NK cell maturation and peripheral homeostasis is associated with KLRG1 up-regulation. J. Immunol. *178*, 4764–4770.

Huntington, N.D., Puthalakath, H., Gunn, P., Naik, E., Michalak, E.M., Smyth, M.J., Tabarias, H., Degli-Esposti, M.A., Dewson, G., Willis, S.N., et al. (2007c). Interleukin 15-mediated survival of natural killer cells is determined by interactions among Bim, Noxa and Mcl-1. Nat. Immunol. *8*, 856–863.

Huntington, N.D., Legrand, N., Alves, N.L., Jaron, B., Weijer, K., Plet, A., Corcuff, E., Mortier, E., Jacques, Y., Spits, H., and Di Santo, J.P. (2009). IL-15 trans-presentation promotes human NK cell development and differentiation in vivo. J. Exp. Med. *206*, 25–34.

Iguchi-Manaka, A., Kai, H., Yamashita, Y., Shibata, K., Tahara-Hanaoka, S., Honda, S., Yasui, T., Kikutani, H., Shibuya, K., and Shibuya, A. (2008). Accelerated tumor growth in mice deficient in DNAM-1 receptor. J. Exp. Med. *205*, 2959–2964.

Joly, E., and Hudrisier, D. (2003). What is trogocytosis and what is its purpose? Nat. Immunol. *4*, 815.

Kim, S., Iizuka, K., Kang, H.S., Dokun, A., French, A.R., Greco, S., and Yokoyama, W.M. (2002). In vivo developmental stages in murine natural killer cell maturation. Nat. Immunol. *3*, 523–528.

Kim, J.M., Rasmussen, J.P., and Rudensky, A.Y. (2007). Regulatory T cells prevent catastrophic autoimmunity throughout the lifespan of mice. Nat. Immunol. *8*, 191–197.

Lakshmikanth, T., Burke, S., Ali, T.H., Kimpfler, S., Ursini, F., Ruggeri, L., Capanni, M., Umansky, V., Paschen, A., Sucker, A., et al. (2009). NCRs and DNAM-1 mediate NK cell recognition and lysis of human and mouse melanoma cell lines in vitro and in vivo. J. Clin. Invest. *119*, 1251–1263.

Lee, G.A., Liou, Y.H., Wang, S.W., Ko, K.L., Jiang, S.T., and Liao, N.S. (2011). Different NK cell developmental events require different levels of IL-15 transpresentation. J. Immunol. *187*, 1212–1221.

Lucas, M., Schachterle, W., Oberle, K., Aichele, P., and Diefenbach, A. (2007). Dendritic cells prime natural killer cells by trans-presenting interleukin 15. Immunity *26*, 503–517.

Mamessier, E., Sylvain, A., Thibult, M.L., Houvenaeghel, G., Jacquemier, J., Castellano, R., Gonçalves, A., André, P., Romagné, F., Thibault, G., et al. (2011). Human breast cancer cells enhance self tolerance by promoting evasion from NK cell antitumor immunity. J. Clin. Invest. *121*, 3609–3622.

Marçais, A., Cherfils-Vicini, J., Viant, C., Degouve, S., Viel, S., Fenis, A., Rabilloud, J., Mayol, K., Tavares, A., Bienvenu, J., et al. (2014). The metabolic checkpoint kinase mTOR is essential for IL-15 signaling during the development and activation of NK cells. Nat. Immunol. *15*, 749–757.

Nabekura, T., Kanaya, M., Shibuya, A., Fu, G., Gascoigne, N.R., and Lanier, L.L. (2014). Costimulatory molecule DNAM-1 is essential for optimal differentiation of memory natural killer cells during mouse cytomegalovirus infection. Immunity *40*, 225–234.

Narni-Mancinelli, E., Chaix, J., Fenis, A., Kerdiles, Y.M., Yessaad, N., Reynders, A., Gregoire, C., Luche, H., Ugolini, S., Tomasello, E., et al. (2011). Fate mapping analysis of lymphoid cells expressing the NKp46 cell surface receptor. Proc. Natl. Acad. Sci. USA *108*, 18324–18329.

Pende, D., Castriconi, R., Romagnani, P., Spaggiari, G.M., Marcenaro, S., Dondero, A., Lazzeri, E., Lasagni, L., Martini, S., Rivera, P., et al. (2006). Expression of the DNAM-1 ligands, Nectin-2 (CD112) and poliovirus receptor (CD155), on dendritic cells: relevance for natural killer-dendritic cell interaction. Blood *107*, 2030–2036.

Ramsbottom, K.M., Hawkins, E.D., Shimoni, R., McGrath, M., Chan, C.J., Russell, S.M., Smyth, M.J., and Oliaro, J. (2014). Cutting edge: DNAX accessory molecule 1-deficient CD8+ T cells display immunological synapse defects that impair antitumor immunity. J. Immunol. *192*, 553–557.

Raulet, D.H. (2004). Interplay of natural killer cells and their receptors with the adaptive immune response. Nat. Immunol. *5*, 996–1002.

Sanchez-Correa, B., Gayoso, I., Bergua, J.M., Casado, J.G., Morgado, S., Solana, R., and Tarazona, R. (2012). Decreased expression of DNAM-1 on NK cells from acute myeloid leukemia patients. Immunol. Cell Biol. *90*, 109–115.

Seth, S., Georgoudaki, A.M., Chambers, B.J., Qiu, Q., Kremmer, E., Maier, M.K., Czeloth, N., Ravens, I., Foerster, R., and Bernhardt, G. (2009). Heterogeneous expression of the adhesion receptor CD226 on murine NK and T cells and its function in NK-mediated killing of immature dendritic cells. J. Leukoc. Biol. *86*, 91–101.

Seth, S., Qiu, Q., Danisch, S., Maier, M.K., Braun, A., Ravens, I., Czeloth, N., Hyde, R., Dittrich-Breiholz, O., Förster, R., and Bernhardt, G. (2011). Intranodal interaction with dendritic cells dynamically regulates surface expression of the co-stimulatory receptor CD226 protein on murine T cells. J. Biol. Chem. *286*, 39153–39163.

Shibuya, A., Campbell, D., Hannum, C., Yssel, H., Franz-Bacon, K., McClanahan, T., Kitamura, T., Nicholl, J., Sutherland, G.R., Lanier, L.L., and Phillips, J.H. (1996). DNAM-1, a novel adhesion molecule involved in the cytolytic function of T lymphocytes. Immunity *4*, 573–581.

Spits, H., Artis, D., Colonna, M., Diefenbach, A., Di Santo, J.P., Eberl, G., Koyasu, S., Locksley, R.M., McKenzie, A.N., Mebius, R.E., et al. (2013). Innate lymphoid cells—a proposal for uniform nomenclature. Nat. Rev. Immunol. *13*, 145–149.

Stanietsky, N., Rovis, T.L., Glasner, A., Seidel, E., Tsukerman, P., Yamin, R., Enk, J., Jonjic, S., and Mandelboim, O. (2013). Mouse TIGIT inhibits NK-cell cytotoxicity upon interaction with PVR. Eur. J. Immunol. *43*, 2138–2150.

Stewart, C.A., Walzer, T., Robbins, S.H., Malissen, B., Vivier, E., and Prinz, I. (2007). Germ-line and rearranged Tcrd transcription distinguish bona fide NK cells and NK-like gammadelta T cells. Eur. J. Immunol. *37*, 1442–1452.

Vesely, M.D., Kershaw, M.H., Schreiber, R.D., and Smyth, M.J. (2011). Natural innate and adaptive immunity to cancer. Annu. Rev. Immunol. *29*, 235–271.

Vivier, E., Tomasello, E., Baratin, M., Walzer, T., and Ugolini, S. (2008). Functions of natural killer cells. Nat. Immunol. *9*, 503–510.

Vosshenrich, C.A., Ranson, T., Samson, S.I., Corcuff, E., Colucci, F., Rosmaraki, E.E., and Di Santo, J.P. (2005). Roles for common cytokine receptor gamma-chain-dependent cytokines in the generation, differentiation, and maturation of NK cell precursors and peripheral NK cells in vivo. J. Immunol. *174*, 1213–1221.

Walzer, T., Bléry, M., Chaix, J., Fuseri, N., Chasson, L., Robbins, S.H., Jaeger, S., André, P., Gauthier, L., Daniel, L., et al. (2007). Identification, activation, and selective in vivo ablation of mouse NK cells via NKp46. Proc. Natl. Acad. Sci. USA *104*, 3384–3389.